J Solid State Electrochem (2011) 15:2083–2094
DOI 10.1007/s10008-011-1399-3

ORIGINAL PAPER

Consistent diffusion coefficients of ferrocene in some non-aqueous solvents: electrochemical simultaneous determination together with electrode sizes and comparison to pulse-gradient spin-echo NMR results

Janina Janisch · Adrian Ruff · Bernd Speiser · Christian Wolff · Jonas Zigelli · Steffi Benthin · Verena Feldmann · Hermann A. Mayer

Received: 25 March 2011 / Accepted: 6 April 2011 / Published online: 12 May 2011

Abstract Cyclic voltammetry data recorded at disk macro- (millimeter dimension) and microelectrodes (10 and 100 μm) at various scan rates are used to simultaneously determine the diffusion coefficient D of ferrocene (fc) and the electroactive surfaces A and/or radii r of the electrodes. A case study with three electrodes of different sizes in CH_3CN- and propylene carbonate (PC)-based electrolytes shows the possibly large effect of incorrect D values. Diffusion coefficients of fc are determined for PC, CH_3CN, CH_2Cl_2, DMF, and DMSO electrolytes and (except for PC) compared to those from pulse-gradient spin-echo nuclear magnetic resonance experiments in the presence of supporting electrolyte in the respective deuterated solvents. The dependence of D_{fc} on solvent viscosity is shown to follow the Stokes–Einstein relation.

Keywords Diffusion coefficients · Electrode size · Ferrocene · Non-aqueous solvents · PGSE NMR spectroscopy

This article is dedicated to Professor Fritz Pragst on the occasion of his 70th birthday.

Electronic supplementary material The online version of this article (doi:10.1007/s10008-011-1399-3) contains supplementary material, which is available to authorized users.

J. Janisch · A. Ruff · B. Speiser (✉) · C. Wolff · J. Zigelli · S. Benthin
Institut für Organische Chemie,
Auf der Morgenstelle 18,
72076 Tübingen, Germany
e-mail: bernd.speiser@uni-tuebingen.de

V. Feldmann · H. A. Mayer
Institut für Anorganische Chemie,
Auf der Morgenstelle 18,
72076 Tübingen, Germany

Introduction

Electrochemical techniques such as cyclic voltammetry or chronoamperometry provide qualitative and quantitative information about electrode processes and coupled chemical reactions [1, 2]. Furthermore, molecular and material characteristics can be derived. This is particularly convenient for diffusion-controlled conditions, where convection and migration are negligible, and kinetic effects are not important.

Since the current i through an electrode depends on the diffusion coefficient D, electrochemical experiments are often used to access this quantity.

Two extreme cases of diffusional transport to disk electrodes, planar and hemispherical diffusion [3, 4], are realized in cyclic voltammetric experiments by selecting appropriate scan rates v for electrodes of particular characteristic dimensions. Thus, if we scan the potential of the electrode fast (high v) and use a large disk electrode (disk radius r in millimeter range), the system is in the planar diffusion regime with peak-shaped current potential curves (transient voltammograms). On the other hand, slow scan rates (small v) and small electrodes (characteristic dimensions ≤20 μm, "ultramicroelectrodes" [4]) lead to hemispherical diffusion with S-shaped steady-state voltammograms. For intermediately sized electrodes, it may be possible to pass from one of these extremes to another by changing the time scale of the experiment through v. The sphericity parameter [4] $\sigma = (D/ar^2)^{1/2}$ with $a = nFv/RT$ (where n is the number of electrons transferred, F is the Faraday constant, R the gas constant, and T the absolute temperature) governs which limiting case is followed: for $\sigma \geq 1$ steady-state voltammograms are obtained, while $\sigma \rightarrow 0$ leads to transient curves. This is rigorously valid only for spherical electrodes. At

disk electrodes, the transition to steady-state behavior may be observed at somewhat higher σ [4].

In both extremes, there are simple relationships between i and D, with Eq. 1 characterizing the planar [5] and Eq. 2 the hemispherical [3, 4] limit.

$$i_p = 0.4463nFAc\sqrt{D}\sqrt{\frac{nF}{RT}v} \quad (1)$$

$$i_{ss} = 4rnDFc \quad (2)$$

In Eq. 1, i_p is the cyclic voltammetric peak current of a reversible (Nernstian) signal (assuming that diffusion is the only transport mode, electrode kinetics are fast, and no chemical reaction steps are coupled to the electron transfer), while $A=\pi r^2$ is the electroactive area of the electrode with radius r and c is the bulk concentration of the electroactive species. In Eq. 2, i_{ss} is the ultramicroelectrode steady-state limiting current.

If v and c are controlled and known, D is determined from the experimental data if n and the electrode size (given by A or r) are available under conditions dictating the use of either Eq. 1 or 2. In fact, any of the three parameters n, D, and r can be determined, provided the other two are known, respectively. For example, a redox couple with previously determined D and a well-defined electrode reaction (n is known) can be used to calibrate the electrode size. This information may then be a prerequisite to further acquire knowledge of D for another compound with known n at the same electrode.

Problems arise if in addition to D, one or more of these quantities is/are inaccessible or known only approximately. We will show first in a case study in this paper that an inaccurate value of the diffusion coefficient can lead to gross inconsistencies in electrode size calibration.

On the other hand, the simultaneous estimation of more than a single one of the possibly unknown parameters in Eqs. 1 and 2 has been described in the literature (see, e.g. Refs. [6–22]) for a variety of situations. In general, both cyclic voltammetry [13, 17, 21] and chronoamperometry [6–16, 18–20, 22] were used. A theoretical treatment concerning the use of microelectrode arrays was also given [23]. In most cases, D and c were determined (in liquid electrolytes [6–8, 16], in ionic liquids [18, 22], in membranes [10, 11], in gels [17], or in the solid state [15, 19]), but simultaneous estimation of D and n has also been described [9, 12, 14, 20].

Electrode sizes and diffusion coefficients were determined simultaneously from such experiments less frequently [13, 16]. While Baur and Wightman [13] combined independent measurements of the electrode radius by scanning electron microscopy with chronoamperometric data, most other estimations rely on the comparison of data under planar and hemispherical conditions. This exploits the fact that D and the other unknowns are related in Eqs. 1 and 2 in different ways. Data evaluation was based in some cases on non-linear parameter optimization techniques [16, 19], correction terms in the diffusion equation [21], or comparison of experimental and simulated (or approximated [24]) chronoamperograms [18]. The two extreme diffusion conditions are most often realized by observation of currents at a single electrode at short and long time scales (variation of v [17] or early and late during chronoamperometry or chronocoulometry [8, 15]).

A second purpose of this paper is to show that such a procedure can not only be conducted by using a single but also several electrodes of different sizes for the investigation of a particular electroactive system by cyclic voltammetry under variation of the scan rate. The single electrode technique requires that the experimental system approaches planar diffusion while still exhibiting a reversible electron transfer at high scan rates and also hemispherical diffusion at slow scan rates. This is not always possible, since finite kinetics (high v) and convection (low v) may limit the scan rate window for diffusion-controlled and reversible behavior. On the other hand, the multi-electrode approach allows to calculate a consistent set of D and all electrode sizes. Heinze [4] discusses the use of electrodes of different sizes for kinetic measurements.

Furthermore, resulting from such estimations, a set of consistent diffusion coefficient values for the commonly used standard redox couple ferrocene/ferricenium ion (fc/fc^+) [25] in various non-aqueous solvents with tetra-*n*-butylammonium hexafluorophosphate (NBu_4PF_6) as supporting electrolyte is provided. Most of these values are additionally confirmed by means of pulse-gradient spin-echo nuclear magnetic resonance (PGSE NMR) [26] spectrometric data. The latter results are determined by a technically totally independent method which does not rely on Faradaic current measurements. Still, the NMR experiments are performed in the same environment as used for the electrochemical experiments, although with deuterated solvents. The NMR samples contain the supporting electrolyte NBu_4PF_6 in the concentration as used in the electrochemical experiments. To our knowledge, diffusion NMR experiments to determine D in the presence of supporting electrolyte have not yet been reported.

Experimental part

Solvents and chemicals

Solvents for electrochemical experiments (DMF, PC, DMSO, CH_3CN, and CH_2Cl_2) were purchased from VWR, Alfa Aesar, J.T. Baker, or Sigma-Aldrich and were of reagent or HPLC grade. $AgClO_4$, NBu_4Br, and NH_4PF_6 were purchased from Alfa Aesar and were of reagent grade. Ferrocene was

obtained from EGA-Chemie (reagent grade). DMF was pre-dried with molecular sieves (3 Å; activated at 400 °C in vacuo over night) for several days prior to distillation. DMF and PC were distilled three times under reduced pressure through a 0.5 m Vigreux column and stored over molecular sieves (3 Å; activated as above) under an argon atmosphere.

CH_3CN and CH_2Cl_2 were pre-dried over $CaCl_2$ before distillation. CH_3CN was distilled successively over P_2O_5, CaH_2, and again P_2O_5. CH_2Cl_2 was first distilled over P_2O_5 and then over K_2CO_3. CH_3CN and CH_2Cl_2 were stored under argon over neutral or basic Al_2O_3, respectively (activated at 230 °C under reduced pressure over night). DMSO (99.97%; Alfa Aesar, HPLC grade, ChemSeal™ bottles, Water 0.01%) was used without further purification.

Dimethylformamide-d_7 (99.5% D), acetonitrile-d_3 (99.8% D), dimethylsulfoxide-d_6 (99.8% D), and dichloromethane-d_2 (99.6% D) were purchased from Merck, Deutero, or euriso-top.

Supporting electrolyte

NBu_4PF_6 was synthesized from NBu_4Br and NH_4PF_6 according to [27]. It was used in a concentration of 0.1 M in the respective solvent as supporting electrolyte.

Electrodes

The following working electrodes were used:

- electrodes A, B1, and C: Pt disk electrodes 6.1204.310 from Metrohm, Filderstadt, Germany, nominal diameter 3±0.1 mm [28].
- electrode B2: 10 μm diameter Pt disk microelectrode MF-2005 from BASi, West Lafayette, IN/USA.
- electrode B3: 100 μm diameter Pt disk microelectrode MF-2150 from BASi, West Lafayette, IN/USA.

Before each use, electrodes A, B1, and C were polished using a suspension of 0.3 μm α-Al_2O_3 powder (Buehler, Lake Bluff, IL/USA) in deionized water. After polishing, the electrodes were rinsed with aceton and deionized water and air-dried. Electrodes B2 and B3 were first washed with ethanol and then with deionized water before and with 0.5 M aqueous NaOH and then water after each experiment.

Electrochemical instruments

For the electrochemical experiments, an Eco-Autolab PGSTAT 100 (Metrohm, Filderstadt, Germany) was used.

Electrochemical procedures

Cyclic voltammograms were recorded at room temperature. All experiments were carried out under argon with a gas-tight full-glass three-electrode cell [27, 29]. The working electrodes are described in "Electrodes" above. The counter electrode was a platinum wire (diameter 1 mm). As potential standard, a Haber-Luggin double reference electrode with a $Ag/AgClO_4$ (0.01 M in 0.1 M NBu_4PF_6/CH_3CN) system [29] was used. All cyclic voltammograms were background corrected. Substrate concentrations were in the range of 0.02–0.4 mM. Appropriate aliquots (30–100 μl) taken from stock solutions (5–10 mM) of fc in the corresponding solvent or electrolyte were used to achieve the desired concentrations. For measurements in CH_2Cl_2, stock solutions of fc were prepared in CH_3CN or PC to avoid evaporation of the volatile CH_2Cl_2 during storage. The addition was carried out using piston-stroke pipettes (Eppendorf, Hamburg, Germany) or a repetitive pipette (Brand, Wertheim, Germany) with positive displacement tips. Electrolytes were degassed by Ar bubbling (PC, CH_3CN, DMF, DMSO) or freeze-pump-thaw procedures (CH_2Cl_2).

NMR experiments

All PGSE NMR experiments were performed on a Bruker Avance II+ 500 spectrometer equipped with a GAB/2 gradient unit and a multinuclear TBO probe with a Z-gradient at a proton resonance frequency of 500.13 MHz. The Bruker stimulated echo pulse sequence stegp1s1d was used. Samples were dissolved in 0.1 M NBu_4PF_6/DMF-d_7, 0.1 M NBu_4PF_6/CD_3CN, 0.1 M NBu_4PF_6/DMSO-d_6, and 0.1 M NBu_4PF_6/CD_2Cl_2 with substrate concentrations of 10–23 mM under an Ar atmosphere, and spectra were recorded at 23 °C without rotation of the NMR tube. To ensure quantitative detection of the fc protons, their longitudinal relaxation time T_1 was determined by the inversion recovery experiment (Bruker pulse sequence t1ir) for each solvent. The delay time between two scans was set to $5T_1$ to ensure complete relaxation.

Computations

Calculations involving non-linear optimization were performed with MATLAB version 7.9 (Mathworks, Inc.) by means of functions `fsolve()` or `lsqnonlin()`. Both functions gave identical results. The Levenberg–Marquardt algorithm was used with Jacobian scaling of the problem.

Results and discussion

A case study: using an inappropriate diffusion coefficient

We will exemplify the problems arising by the use of an inappropriate diffusion coefficient for the determination of the electroactive area of an electrode by reporting the results

of some experiments to calibrate the size of a commercial Pt disk electrode (electrode tip). The nominal diameter of the Pt disk is 3 mm (electrode A) [28]. The electrode was intended to be used in the following procedure:

1. Calibrate the electroactive area A with cyclic voltammetric peak current data of ferrocene in acetonitrile, based on a diffusion coefficient $D_{fc}(CH_3CN)=2.4\times10^{-5}$ cm^2 s^{-1} taken from ref. [30]. In this step, it is assumed that the exact electrolyte composition, in particular the identity and concentration of the supporting electrolyte (0.1 M NBu_4PF_6 in the present work, 0.2 M $LiClO_4$ in ref. [30]), does not significantly influence D.
2. Under the reasonable assumption that A does not depend on the electrolyte composition, use the calibrated area to determine D for ferrocene in a propylene carbonate (PC) electrolyte, D_{fc}(PC).
3. Use D_{fc}(PC) to calibrate other electrodes with respect to A or r by experiments in PC.

A literature survey for D_{fc}(PC) determined by cyclic voltammetry reveals a range of values, measured under different conditions (Table 1), and both the type and the concentration of the supporting electrolyte seem to have a considerable (albeit not easily understood) influence. Furthermore, the water content of the sample seems to slightly change the value of the diffusion coefficient. Thus, it was deemed necessary for quantitative work to use a value for D_{fc}(PC) determined under our electrolyte conditions.

For calibration, four independent experiments with the acetonitrile electrolyte (independently prepared stock solutions of fc; three or four concentrations by addition of defined volumes of the respective stock solution per experiment) were conducted under variation of the scan rate using electrode A. The peak potential differences ΔE_p are only slightly above the theoretical value of 58 mV, and almost independent of c and v (see Supporting information), indicating the absence of kinetic effects and significant iR drop in almost the entire range investigated. The peak currents are proportional to $\sqrt{vc}$ over a wide range of v and c indicating planar diffusion-controlled behavior. To avoid the influence of convection at low v (<0.05 Vs^{-1}; increase of $i_p/\sqrt{vc}$) and electrode kinetics at high v (>1 Vs^{-1}; increase of ΔE_p, decrease of $i_p/\sqrt{vc}$) only peak current data for $0.05\le v\le1$ Vs^{-1} were used for the evaluation of A (see Table 2 for data from a particular experiment). There is a slight tendency for decreasing normalized peak currents with increasing v and decreasing c. However, all values are within about 5% of the mean value, which is a common estimate for the reproducibility of current measurements (see, for example the estimation of the accuracy of experimental determinations of n [31, 32]). From all independent experimental data sets in the study, a mean of $A_A=0.079\pm0.002$ cm^2 was calculated. This value is somewhat above that derived from the specification of the diameter as given by the supplier [28]. However, this could easily be explained by some scratches and/or surface roughness introduced by extensive previous use of this particular electrode.

Table 1 Selected literature values for D_{fc} (PC)

Source	D_{fc}(PC) $\times10^6$/cm^2 s^{-1}	Electrolyte
[33]	3.0	$NaClO_4$ (0.5 M), 0.2% H_2O
[33]	3.4	$NaClO_4$ (0.5 M), 5% H_2O
[44]	4.4	NEt_4ClO_4 (0.1 M)
[45]	5.6±0.1	$LiClO_4$ (0.1 M)
[46]	6.5±0.2	$LiClO_4$ (0.1 M)
[47]	7–6	$NaClO_4$ (0.1 M), 0.2–5% H_2O

In the second step of the study, six independent experiments with four concentrations of fc each in propylene carbonate were performed. Selected current results are also collected in Table 2. They show similar characteristics as the CH_3CN data with a smaller degree of normalized current variation with v and c. Application of Eq. 1 and A (as determined in CH_3CN before) results in a diffusion coefficient $D_{fc}(PC)=2.8\pm0.1\times10^{-6}$ cm^2 s^{-1}. This is slightly below the lower limit of the values reported in the literature. However, given the considerable variation of the results in Table 1, it does not appear to be unreasonable.

Note that in the use of the propylene carbonate result for further studies at macroelectrodes, any errors in the *absolute* value will go undetected, since we are only able to analyze *relative* current data, as Amatore and coworkers have convincingly argued for the determination of electron stoichiometry [12].

Subsequently, we used the above value of D_{fc}(PC) to calibrate the electroactive area of additional planar disk electrodes with fc electrolytes. In this part of the work, not only another specimen of the 3 mm diameter electrodes, electrode B1, but also two microelectrodes[1] of commercial origin were included, i.e., a d=10 μm (B2) and a d=100 μm (B3) Pt disk electrode (nominal diameters). According to the supplier of B2 and B3, the disk diameters are accurate to ±10% (Howell, Bioanalytical Systems, Inc., personal communication 2010). Electrodes B1–B3 were calibrated by means of cyclic voltammograms in the planar diffusion regime (electrode B1; electrode B3 at faster scan rates) and in the steady-state region (electrode B2; electrode B3 at slower scan rates). Since the sphericity is only approximate for planar electrodes [4], it was additionally checked in the experiments that $i_p^{ox}/\sqrt{vc}$ was independent

[1] In the following, we will use the term "microelectrode" not only for electrodes conforming to Heinze's definition ($d\le20$ μm) [4] but also for those of a larger diameter if used under conditions where a hemispherical diffusion steady-state can be achieved.

Table 2 Normalized peak currents $i_p^{ox}/\sqrt{v}c$ in $\mu A\, s^{1/2}\, mV^{-1/2} mM^{-1}$ for fc in CH_3CN and PC at electrode A

v/V s^{-1}	$i_p^{ox}/\sqrt{v}c$							
	c(fc)/mM[a]				c(fc)/mM[b]			
	0.049	0.064	0.123	0.180	0.102	0.196	0.281	0.360
0.05	3.22	3.30	3.35	3.41	1.07	1.10	1.11	1.12
0.07	3.19	3.25	3.32	3.39	1.08	1.10	1.11	1.12
0.1	3.17	3.23	3.30	3.36	1.07	1.10	1.11	1.12
0.2	3.14	3.20	3.28	3.33	1.07	1.10	1.11	1.12
0.5	3.08	3.13	3.21	3.29	1.07	1.09	1.11	1.11
0.7	3.10	3.14	3.23	3.28	1.06	1.09	1.11	1.11
1.0	3.08	3.16	3.22	3.28	1.07	1.10	1.11	1.11

[a] In CH_3CN/0.1 M NBu_4PF_6

[b] In PC/0.1 M NBu_4PF_6

of v for the planar conditions. Furthermore, it was ensured that i_{ss} was independent of v and that the curves recorded at low v did not show a peak feature or considerable hysteresis effect for the forward and reverse scan in the hemispherical diffusion experiments. Typical results in Table 3, however, show a suspicious inconsistency between data from planar and hemispherical diffusion conditions: while the electroactive area for B1, A_{B1}, and the radius r_{B3} at high scan rates are only slightly larger than expected from the manufacturers' specifications, r_{B2} and r_{B3} (at small v) show deviations of ≈40% and more, significantly outside the tolerances. At this point, an incorrect value of D_{fc}(PC) was suspected. Indeed, when employing various hypothetical D_{fc}(PC) (see Supporting information) for selected data of electrode B3 at low and high v, the results became increasingly more consistent with increasing values of the diffusion coefficient. Around $D_{fc}(PC)=4.0\times10^{-6}$ cm^2 s^{-1}, they converge to within one standard deviation. The use of such a higher value in the calculation of r_{B2} and A_{B1} also gave consistent results. This case study clearly shows that incorrect estimates of the diffusion coefficient can have a surprisingly large effect on quantitative absolute electrochemical data. If one works with either macro- or microelectrodes in their planar or hemispherical diffusion regime only, the resulting erroneous values may go undetected and might influence further data analysis. Only the combined data from both diffusion types allow the detection of such errors through obvious inconsistencies and their correction. The reason for the incorrect D_{fc}(PC) may partially be traced back to an incorrect $D_{fc}(CH_3CN)$, but any additional experimental error, e.g., related to concentration or current measurement, will possibly further increase the derivation from the true value.

Table 3 Electrode area and/or radius for electrodes B1–B3 from cyclic voltammetric experiments in PC/0.1 M NBu_4PF_6 (fc solution) under the assumption $D_{fc}(PC)=2.8\times10^{-6}$ cm^2 s^{-1} in typical experiments, mean values over several concentrations as indicated

Electrode	v/V s^{-1}	A/cm^2	r/μm
B1[a,b]	0.05	0.079	–
	0.5	0.079	–
	5.04	0.076	–
B2[c,d]	0.001	–	7.0
	0.002	–	7.0
	0.005	–	7.0
B3[b,d]	0.001	–	72.5
	0.002	–	71.5
	1.0	–	55.5
	1.993	–	54.5

[a] Nominal area: $A_{nom}=0.0707\pm0.0004$ cm^2, the error in A_{nom} is estimated from the specification [28] assuming Gaussian error propagation

[b] Four concentrations

[c] Six concentrations

[d] Nominal radius see "Experimental part"

Simultaneous determination of D and A or r in PC/0.1 M NBu_4PF_6

The severe problem originating from the fact that the current through an electrode varies with both the diffusion coefficient of the redox-active species and the electrode size can possibly be solved by including in the analysis a combination of planar and hemispherical diffusion data. Under advantageous circumstances, it might even be possible to generate these data from a single electrode of intermediate size. We will use such a system (fc in PC) first to demonstrate two alternatives of data evaluation (explicit calculation and non-linear optimization). The analysis of data from two (or more) different electrodes will be shown also.

Sphericity effects on fc voltammograms in propylene carbonate experiments

The use of electrode B3 for cyclic voltammetric experiments with fc in PC demonstrates that the redox system fc/fc^+ can be driven close to both planar and hemispherical diffusion

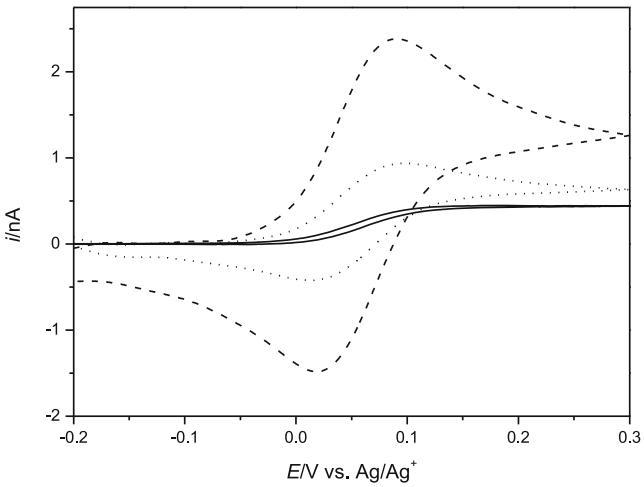

Fig. 1 Cyclic voltammograms of fc at electrode B3 in PC/0.1 M NBu_4PF_6, c=0.054 mM, v=0.001 Vs^{-1} (*solid line*), 0.1 Vs^{-1} (*dotted line*), 1 Vs^{-1} (*dashed line*)

conditions leading to transient or steady-state i/E curves at higher or lower scan rates, respectively (Fig. 1).

While at 1 Vs^{-1}, a reversible peak-shaped voltammogram is obtained (ΔE_p=72 mV, $i_p^{red}/i_p^{ox} = 0.964$), the i/E curve at 0.1 Vs^{-1} shows a mixed form, and the one at 0.001 Vs^{-1} is a typical S-shaped steady-state voltammogram with only minor deviations between forward and reverse trace. Furthermore, for scan rates of 1.0 and 1.993 Vs^{-1}, i_p^{red}/i_p^{ox} stays close to unity and the normalized current $i_p^{ox}/\sqrt{v}c$ is constant as expected for a diffusion controlled process. For v>2 Vs^{-1}, some effects of electrode kinetics become apparent. The steady-state behavior is attained for v=0.001 and 0.002 V s^{-1}. For v>0.002 Vs^{-1}, the superposition of the forward and the reverse scan starts to show increasing hysteresis. Based on these results, it was concluded that electrode B3 could possibly be used for the simultaneous determination of D_{fc}(PC) and r_{B3} with slow and fast scan rate data. The results are compared to those from experiments with B1 and B2 only, where clearly planar and hemispherical diffusion conditions are achieved, respectively.

Cyclic voltammetry current analysis

We applied two types of analysis to determine D and the electrode sizes simultaneously from experimental cyclic voltammetry data.

Either, Eqs. 1 and 2 are combined to eliminate the electrode radius (noting $A=\pi r^2$) and arrive at D as the only unknown, Eq. 3 (after resolving the numerical constants).

$$D = \sqrt[3]{\frac{0.007679}{nFRT}\left(\frac{(i_{ss}/c)^2}{i_p^{ox}/\sqrt{v}c}\right)^2} \tag{3}$$

The derivation of this equation assumes that both hemispherical and planar diffusion conditions can be reached with a single electrode. It is particularly convenient, since the values of the currents normalized by c or $\sqrt{v}c$ are usually calculated to check the validity of assumptions such as diffusion control of the process. After D has been determined, any of the Eqs. 1 and 2 can be used to calculate r and consequently A. We will call this the "explicit calculation" of D and r.

Alternatively, if the conditions necessary to derive Eq. 3 cannot be reached and the two types of diffusion are realized at two or more electrodes with different sizes, the non-linear optimization problem presented by Eqs. 4 and 5 must be solved.

$$R_{hs,m_1} = \left(i_{ss}/c - 4r_j nFD\right)/(i_{ss}/c) \tag{4}$$

$$R_{pl,m_2} = \left(i_p/\sqrt{v}c - 0.4463nF\left(\pi r_k^2\right)\sqrt{DnF/RT}\right)/\left(i_p\sqrt{v}c\right) \tag{5}$$

Here, we assume that we have m_1+m_2 individual determinations of currents, m_1 under hemispherical (hs) and m_2 under planar (pl) diffusion conditions. For each of these experiments, we calculate the normalized residual R between the experimental current and the current calculated with values of D and the radii r of the electrodes. The normalization is necessary since steady-state currents i_{ss} and transient peak currents i_p may attain values of strongly different sizes.

Equations 4 and 5 correspond to an overdetermined system of non-linear equations with the unknowns D as well as r_j and r_k (j=1,…, l_{hs}, for l_{hs} electrodes with hemispherical and k=1,…, l_{pl}, for l_{pl} electrodes with planar diffusion conditions). The unknowns are optimized such that the sum of squared residuals is minimized. Thus, this technique allows the estimation of all unknowns even if the hemispherical and planar diffusion conditions are reached

Table 4 Determination of D_{fc} (PC) and sizes r of electrodes B1–B3 from cyclic voltammetric experiments in PC/0.1 M NBu_4PF_6

Method	Electrodes	D_{fc}(PC)×10^6/cm^2s^{-1}	r_{B1}/mm	r_{B2}/mm	r_{B3}/mm
Explicit	B1–B3	4.1±0.2	1.44±0.02	0.00473±0.00006	0.05±0.001
Non-linear	B1–B3	4.1±0.1	1.44±0.01	0.0047±0.0001	0.050±0.0006
Non-linear	B1, B2	3.87±0.02	1.457±0.009	0.00501±0.00005	–

Table 5 Diffusion coefficients D_{fc} (DMF) as reported in the literature (selected references) and determined in this work

Source	D_{fc}(DMF) $\times 10^5$ /cm^{2}s^{-1}	System/method[a]
[33]	0.57	Pt, CV, 0.5 M $NaClO_4$: 21% (*v*/*v*) H_2O
[35]	≈0.9[b]	Au (see [48]), CV, 0.1 M NBu_4ClO_4
[43]	0.95±0.02	Pt, CV, 0.1 M NBu_4PF_6
[34]	0.97	Pt-RDE, 0.1 M NBu_4ClO_4, c=0.1–1.5 mM, ω=1,000 rpm
[36]	0.98	Pt, microelectrode voltammetry, 0.1 M NBu_4PF_6
[21]	1.0±0.1	Pt, CV, 0.1 M NBu_4ClO_4, T=26 °C
[37]	1.07±0.04	Pt, steady-state microelectrode flow cell, 0.1 M NBu_4ClO_4, T=24.8 °C
[33]	1.1	Pt, CV, 0.5 M $NaClO_4$
This work	1.07±0.06[c]	Electrode B3
This work	1.07[d]	Electrode B3
This work	1.06±0.01[e]	PGSE NMR spectroscopy, 0.1 M NBu_4PF_6, DMF-d_7, T=23 °C

[a] *RDE* rotating disk electrode, *CV* cyclic voltammetry

[b] Approximate value taken from Fig. 3 in ref. [35]

[c] Explicit simultaneous determination of D_{fc}(DMF) and r_{B3}

[d] Non-linear estimation of D_{fc} (DMF) and r_{B3}=0.05 mm

[e] Mean value from three determinations, c=10.75–12.4 mM

at different electrodes, and furthermore the determination of several electrode sizes together with D.

Explicit calculation of D and r was used for data recorded at electrode B3 (v=1.0 and 1.993 Vs^{-1} for planar, v=0.001 and 0.002 Vs^{-1} for hemispherical diffusion; five independent experiments with a total of 15 concentrations between 0.0534 and 0.2191 mM). After determination of D_{fc}(PC) and r_{B3}, Eqs. 1 and 2 were used to calculate r_{B1} and r_{B2} (row 1 in Table 4) from current data recorded at these electrodes. This analysis confirms that D_{fc}(PC) is significantly higher than the value determined in the case study and that the electrode sizes are rather close—albeit not identical—to the nominal values.

Non-linear estimation of D_{fc}(PC) from the data (row 2 in Table 4) results in values almost identical to those determined by Eq. 3. Here, the standard deviation is approximated by separately estimating the D and r from five independent B3 experiments (several concentrations each) combined with B1 and B2 data. The standard deviations given are calculated from the resulting five estimation results.

As discussed before, with electrode B3, it is only possible to reach planar and hemispherical diffusion conditions approximately. Any influence of this fact could be eliminated by restricting the analysis to data from B1 and B2 (row 3 in Table 4). The σ values for B1 (0.000478 for v=0.02 Vs^{-1}) and B2 (6.4114 for v=0.01 Vs^{-1}) show that the planar transient and hemispherical steady-state cases can clearly be achieved even for relatively slow or fast scan rates, respectively. In this case, the analysis is only possible with the non-linear optimization method, which yields a slightly lower value for the diffusion coefficient and slightly higher radii for B1 and B2. The values for r_{B1} and r_{B2} are closer to the respective nominal values. For the further discussion, D_{fc}(PC) determined from B1 and B2 data will be used.

A consistent set of diffusion coefficients for ferrocene in some non-aqueous electrolytes

The propylene carbonate data, as analyzed in the previous section, allow to simultaneously determine a diffusion coefficient D_{fc}(PC) and various electrode sizes. This set of results will now be used to extend the determination to other electrolytes (based on DMF, CH_3CN, CH_2Cl_2, and DMSO as solvents), where planar and hemispherical diffusion may not be attained easily at an intermediately sized electrode disk. In some cases, the previously determined electrode sizes were used to allow the calculation of D_{fc}. We will compare the

Table 6 Normalized current data for fc in DMF/0.1 M NBu_4PF_6 at electrode B3 in a typical experiment

	Concentration c/mM			
	0.0223	0.0444	0.0664	0.0881
Scan rate				
v/V s^{-1}	i_{ss}/c[a]	i_{ss}/c[a]	i_{ss}/c[a]	i_{ss}/c[a]
0.001	20.66	20.21	20.74	20.28
0.002	21.20	21.55	20.96	20.73
0.005	21.53	21.58	21.08	20.95
Scan rate				
v/V s^{-1}	$i_p^{ox}/\sqrt{v}c$	$i_p^{ox}/\sqrt{v}c$	$i_p^{ox}/\sqrt{v}c$	$i_p^{ox}/\sqrt{v}c$
0.5	2.586	2.607	2.568	2.553
1.0	2.339	2.370	2.349	2.343
1.993	2.240	2.284	2.248	2.235

[a] In nA mM^{-1}

[b] In μA s$^{1/2}$ mV$^{1/2}$ mM^{-1}

results to values from the literature, although these are usually generated under varying conditions, in particular with different electrolyte compositions and to NMR results.

Diffusion coefficient of ferrocene in DMF/0.1 M NBu_4PF_6

Values of D_{fc}(DMF) as reported in the literature [21, 33–37] are rather consistent around 1×10^{-5} cm^2 s^{-1} (Table 5). Only a high water content seems to decrease the value [33] by a significant amount.

The higher value compared to D_{fc}(PC) indicates that it might become difficult to reach the planar diffusion limit at the d=100 μm disk electrode. Indeed, σ=0.0103 for v=1 V s^{-1}, while σ=2.05 for v=0.005 Vs^{-1}. Thus, steady-state behavior is expected even for scan rates as high as 0.005 V s^{-1}. On the other hand, the cyclic voltammograms for v=0.5 and 1.0 Vs^{-1} at electrode B3 show a peak current ratio i_p^{red}/i_p^{ox} which clearly deviates from unity, leading us to exclude data at these scan rates from the analysis. At the same time, we have to avoid artifacts generated by electron transfer kinetics at scan rates above 2 Vs^{-1}. Consequently, only data at v=1.993 Vs^{-1} were used for the calculations (data from a particular experiment, see Table 6). Here, i_p^{red}/i_p^{ox} has reached unity with only a very small deviation. The peak current data at v=1.993 Vs^{-1} were combined in the explicit calculation scheme with i_{ss} at v=0.001, 0.002, and 0.005 Vs^{-1}, which results in D_{fc}(DMF)=1.07±0.06×10^{-5} cm^2 s^{-1} and a radius r_{B3}=0.050±0.001 mm, the latter being in close agreement with the PC experiment results.

Inclusion of the v=0.5 and 1.0 Vs^{-1} data results in increasing deviations from r_{B3} determined with the PC data. At the same time, the value of D_{fc}(DMF) decreases (see Supporting information). This clearly indicates that the analysis excluding these values is optimal and the diffusion coefficient is reliable, since the electrode radius should not change with the solvent. Non-linear estimation of D_{fc}(DMF) and r_{B3} resulted also in consistent values (Table 5).

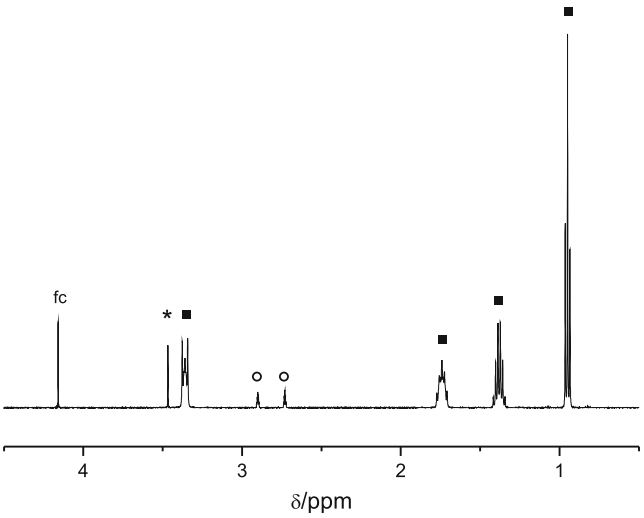

Fig. 2 ^{1}H NMR spectrum of fc in 0.1 M NBu_4PF_6/DMF-d_7 (c= 10.75 mM); (*filled square*) NBu_4PF_6, (*empty circle*) solvent, (*star*) residual water; without field gradient

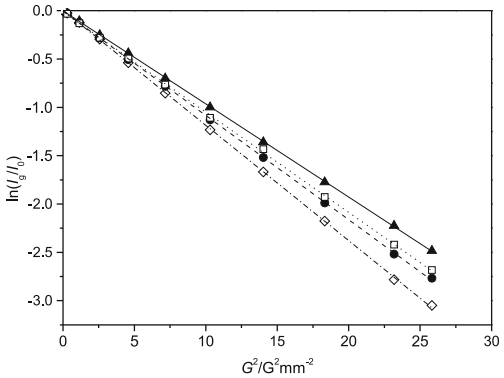

Fig. 3 Logarithmic analysis of the normalized peak area as a function of the squared magnetic field gradient from exemplary PGSE NMR experiments with fc in (*empty diamond*) CD_3CN (c_{fc}=13.10 mM, R^2=0.9999), (*solid circle*) DMF-d_7 (c_{fc}=10.75 mM, R^2=0.9999), (*empty square*) CD_2Cl_2 (c_{fc}=11.60 mM, R^2=0.9997) and (*solid triangle*) DMSO-d_6 (c_{fc}=11.70 mM, R^2=0.9999)

According to the theory of PGSE NMR spectroscopy [38, 39], the peak area of an NMR signal depends on the magnetic field gradient G. The ratio of the integrals in the absence (I_0) and presence (I_g) of such a gradient depends on the diffusion coefficient, Eq. 6.

$$\ln\left(I_g/I_0\right) = -\left[\gamma^2\delta^2G^2(\Delta-\delta/3)\right]D \qquad (6)$$

where γ is the magnetogyric ratio of the ^{1}H nucleus, δ is the pulse width of the gradient pulse, and Δ is the time between two gradient pulses. D_{fc}(DMF) was determined by integration of the ^{1}H signals of the fc protons and the slopes of ln

Table 7 Ferrocene diffusion coefficient in DMF-d_7 from PGSE NMR data

c/mM	D_{fc}(DMF) ×10^5/cm^{2}s^{-1}	R^2 [a]
10.75[b]	1.05	0.9999
10.75[b]	1.07	0.9996
12.40	1.07	0.9994

[a] R^2 obtained from the graphical analysis of ln(I_g/I_0) vs. G^2 (R is the correlation coefficient)

[b] Repetition experiments

Table 8 Diffusion coefficients D_{fc} (CH_3CN) as reported in the literature (selected references) and determined in this work

Source	$D_{fc}(CH_3CN)$ $\times 10^5/cm^2s^{-1}$	System/method[a]
[35]	≈1.2	Au (see [48]), CV, 0.1 M NBu_4ClO_4[b]
[49]	1.85	Pt/glassy carbon, CV, 0.1 M NBu_4PF_6
[50]	2.1	CA, 5–100 mM, 0.5 M NBu_4ClO_4
[34]	2.2	Pt-RDE, 0.1 M NBu_4ClO_4, c=0.1–1.5 mM, ω=1,000 rpm
[43]	2.24±0.06	Pt, CV, 0.1 M NBu_4PF_6
[42]	2.28±0.04	Glassy carbon, CA, 0.1 M NBu_4PF_6
[37]	2.37±0.1	Pt, flow cell, 0.1 M NBu_4ClO_4, 24 °C
[30]	2.4	chronopotentiometry, Pt, 0.2 M $LiClO_4$
[40]	2.6	glassy carbon, CV, 1–500 mM NBu_4ClO_4
This work	2.5±0.1	Electrodes B1 and B2, Eqs. 1 and 2
This work	2.47[c]	Electrodes B1 and B2, non-linear estimation
This work	2.53±0.06[d]	PGSE NMR spectroscopy, 0.1 M NBu_4PF_6, CD_3CN, T= 23 °C

[a] *RDE* rotating disk electrode, *CV* cyclic voltammetry, *CA* chronoamperometry

[b] Approximate value taken from Fig. 3 in ref. [35]

[c] Simultaneous estimation of r_{B1}= 1.45 mm and r_{B2}=0.005 mm

[d] Mean value from five independent experiments, c=12–22.6 mM

(I_g/I_0) versus G^2 plots (Fig. 3). The results prove to be highly reproducible (Table 7).

Although the concentrations in the NMR experiments were higher than those in the electrochemical ones owing to sensitivity reasons, both techniques result in practically the same value of D_{fc}(DMF), further confirming the validity of the results. The value is close to those reported in the literature (Table 5). The system fc in DMF is at the limit of applicability of the single electrode explicit determination of D and r. Still, the analysis appears to provide a sensible value.

Diffusion coefficient of ferrocene in CH_3CN/0.1 M NBu_4PF_6

As in the case of PC electrolytes, the literature reports on $D_{fc}(CH_3CN)$ differ considerably (Table 8). The diffusion coefficient in this solvent, however, seems to be considerably larger than in PC and DMF. Thus, we expect to be outside the range of D_{fc} where we can reach planar and hemispherical diffusion behavior with the same electrode (B3) without incurring kinetic effects on the peak current. Indeed our experiments show that even at v=1.993 Vs^{-1}, the peak current ratio has not yet reached values close to unity. At the same time, however, the peak potential difference ΔE_p starts to increase indicating quasi-reversibility effects. Consequently, the simultaneous explicit estimation of D and r was not possible.

However, the value of $D_{fc}(CH_3CN)$ (Table 8) was determined electrochemically at electrodes B1 ($0.05 \le v \le 0.5$ Vs^{-1}, $0.049 \le c \le 0.206$ mM; planar diffusion conditions; two independent experiments, eight concentrations) and B2 ($0.001 \le v \le 0.02$ Vs^{-1}, $0.057 \le c \le 0.272$ mM; hemispherical diffusion conditions; two independent experiments, nine concentrations). For the data evaluation by means of Eqs. 1 and 2, the electrode sizes were assumed to be those determined in the PC- and DMF-based electrolytes before. The results are confirmed by the simultaneous estimation of $D_{fc}(CH_3CN)$ and the electrode sizes by non-linear optimization. Again, the value from PGSE NMR experiments matches that from the electrochemical experiments closely (Table 8, last entry). These results are close to the upper limit [40] as reported in the literature. It might be speculated that the small values reported in some cases may be due to effects of the electron transfer kinetics, which decreases the current and thus D when applying the Nicholson and Shain [5] relation. In the present work, care

Table 9 Diffusion coefficients D_{fc} (CH_2Cl_2) as reported in the literature (selected references) and determined in this work

Source	$D_{fc}(CH_2Cl_2)$ $\times 10^5/cm^2s^{-1}$	System/method[a]
[43]	1.67±0.05	Pt, CV, 0.1 M NBu_4PF_6 , 298.15 K
[34]	1.7	Pt-RDE, 0.1 M NBu_4ClO_4, c=0.1–1.5 mM, ω=1,000 rpm
[51]	1.8	Au, CC, 0.1 M NBu_4BF_6
[52]	1.92	Pt, CV, 0.1 M NBu_4BF_6
[53]	2.1	Glassy carbon, CV, 0.05 M $NBu_4B(C_6F_5)_4$
[54]	2.32±0.1	Pt, microelectrode, 0.1 M NBu_4ClO_4, c=0.5 mM
This work	2.2±0.1	Electrodes B1, C, and B2; Eqs. 1 and 2
This work	2.1[b]	Electrodes B1, C, and B2; non-linear estimation
This work	2.4±0.2[c]	PGSE NMR spectroscopy, 0.1 M NBu_4PF_6 , CD_2Cl_2, T=23 °C

[a] *RDE* rotating disk electrode, *CV* cyclic voltammetry, *CC* chronocoulometry

[b] Simultaneous estimation of r_{B1}=1.46 mm, r_C=1.47 mm, and r_{B2}=0.005 mm

[c] Mean value from four independent experiments, c=11.6–12.6 mM

Table 10 Diffusion coefficients D_{fc} (DMSO) as reported in the literature (selected references) and determined in this work

[a] *RDE* rotating disk electrode, *CV* cyclic voltammetry, *CA* chronoamperometry, *CC* chronocoulometry

[b] Mean value from three independent experiments, c=11.7 mM

Source	D_{fc}(DMSO) $\times 10^6$/ $cm^2 s^{-1}$	System/method[a]
[34]	4.4	Pt-RDE, 0.1 M NBu_4ClO_4, c=0.1–1.5 mM, ω=1,000 rpm
[43]	4.4±0.1	Pt, CV, 0.1 M NBu_4PF_6
[55]	6.7	Pt, CA/CC, 0.1 M NBu_4PF_6
This work	4.9±0.1	Electrodes B1 and B2, Eqs. 1 and 2
This work	4.7±0.1	Electrode B1 and B2, non-linear estimation
This work	4.69±0.03[b]	PGSE NMR spectroscopy, 0.1 M NBu_4PF_6, DMSO-d_6, T=23 °C

was taken to restrict planar diffusion data to conditions where such kinetic effects could be assumed to be mostly absent (independence of normalized peak currents and ΔE_p from scan rate).

The values determined from electrochemical and NMR data are slightly above the reference value used in the case study discussed in the first part of this paper. This confirms that at least some part of the inconsistency noted when using different electrode sizes was due to an inaccurate $D_{fc}(CH_3CN)$. It would, however, not account for the full deviation of D_{fc}(PC) calculated using $D_{fc}(CH_3CN)$ from ref. [30].

Diffusion coefficient of ferrocene in CH_2Cl_2/0.1 M NBu_4PF_6

Again, values for $D_{fc}(CH_2Cl_2)$ reported in the literature show significant variation (Table 9). Nevertheless, it is roughly close to that of $D_{fc}(CH_3CN)$, and we expect a similar behavior as regards the use of electrode B3 in acetonitrile. Thus, electrodes B1 and B2 were employed in the experiments only. Some data were recorded with an electrode C (same type as B1).

A total of 26 different concentrations ($0.02 \le c \le 0.2$ mM) were used in eight independent experiments, and planar diffusion was achieved at B1 (or C) for $0.05 \le \nu \le 1.0$ Vs^{-1}, while hemispherical diffusion was apparent at electrode B2 for $0.001 \le \nu \le 0.01$ Vs^{-1}. Results from the use of Eqs. 1 and 2 assuming the electrode radii determined earlier on one hand and from the simultaneous non-linear estimation of $D_{fc}(CH_2Cl_2)$ and the electrode dimensions on the other, agree well (Table 9). As in the other cases, our diffusion coefficient is close to the upper limit of the literature reference values. The value determined by PGSE NMR spectroscopy is even slightly higher. However, still the standard deviations clearly overlap. In fact, the standard deviation of the NMR value is unusually high as compared to the other solvents investigated in this work. A possible difficulty in using CH_2Cl_2-based electrolytes at room temperature is the high vapor pressure of this solvent, which makes handling tedious. Concentrations may be less reliable when preparing the solutions in CH_2Cl_2 as compared to less volatile solvents. The non-linear size estimation is consistent with the results in PC and DMF, again confirming the reliability of the results.

Diffusion coefficient of ferrocene in DMSO/0.1 M NBu_4PF_6

Compared to other non-aqueous solvents, there are few values for D_{fc}(DMSO) in the literature (Table 10). They differ strongly by a factor of ≈1.5. In the present work, electrochemical data were recorded with electrodes B1 (planar diffusion; $0.05 \le \nu \le 1.0$ Vs^{-1}; five independent experiments; 17 concentrations) and B2 (hemispherical diffusion; $0.001 \le \nu \le 0.01$ Vs^{-1}; five concentrations). Concentrations were between 0.053 and 0.274 mM. Under the assumption of the previously determined electrode sizes, it can be shown that D_{fc}(DMSO) from these data is close to the lower limit of the literature reference values. This is confirmed by the result of non-linear estimation, which also gives electrode sizes (r_{B1}=1.47 mm and r_{B2}= 0.005 mm) that are consistent with the results from the other solvents used in this study.

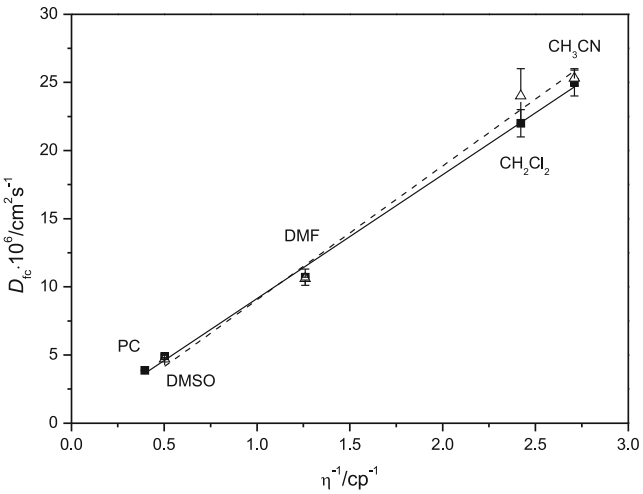

Fig. 4 Dependence of D_{fc} on dynamic solvent viscosity η for the solvents used in this work; (*filled square*) D obtained from CV experiments by explicit calculation (PC, DMF) or use of Eqs. 1 and 2 (CH_3CN, CH_2Cl_2, DMSO), (*empty triangle*) D obtained from PGSE NMR experiments; *error bars* give standard deviations (σ). *Solid line*: linear regression of D(CV), R^2=0.9969; *dashed line*: linear regression of D(NMR), R^2=0.9876. Dynamic viscosities are for the pure non-deuterated solvents at 25 °C (without supporting electrolyte) [56]

Solvent effects on the diffusion coefficient of ferrocene

It is well known that D correlates linearly with the reciprocal of the dynamic solvent viscosity η (Stokes–Einstein relation [41]):

$$D = \frac{k_B T}{6\pi\eta r} \quad (7)$$

where k_B is the Boltzmann constant and r is the hydrodynamic radius of the diffusing molecule. This behavior is clearly shown for the D_{fc} determined in the five non-aqueous solvents in this work (Fig. 4). Electrochemical results from either explicit calculations (if the necessary conditions could be met; PC, DMF) or the use of Eqs. 1 and 2 and separately determined electrode radii (CH_3CN, CH_2Cl_2, DMSO) are included in the graph. They compare very well to the diffusion NMR results (also in Fig. 4), showing that the concentrations of fc were low enough to make diffusion under a concentration gradient (electrochemical experiments) and self-diffusion (NMR experiments) equivalent [42]. The experimental standard deviations are very small for the PC and DMSO data. In DMSO and CH_2Cl_2, the relative deviation between the electrochemically and the spectroscopically determined D_{fc} is largest, but still reasonable if the standard deviations are considered. The consistency of the electrode radii determined in this work from the electrochemical data in all electrolytes, as discussed in previous sections, corroborates the validity of the D_{fc}.

Thus, the D_{fc} in the five non-aqueous electrolytes prove to be highly reliable over a factor of ≈5, similar to the data in ref. [43] with a different set of solvents. However, for those solvents used in both studies, our values seem to be consistently higher.

Conclusion

The determination of ferrocene diffusion coefficients in five non-aqueous electrolytes results in a consistent set of values cross-checked with PGSE NMR spectroscopic data recorded in the presence of supporting electrolyte. Only in PC, this check was impossible because the NMR signal of fc is obscured by the solvent resonance. The D_{fc} correlates well with the dynamic solvent viscosity. However, the electrochemical determination critically depends on the availability of data in both the hemispherical and planar diffusion regimes. If electrode sizes (or concentrations) are inaccurately known, lack of data for one of these conditions possibly results in erroneous values of D. Another important aspect is the exclusion of current data that may be affected by electrode kinetics at high scan rates.

Two alternative calculation techniques are presented for the case when steady-state and transient voltammetry can be performed with either a single or more than one electrode(s) (explicit determination, non-linear optimization) and shown to produce comparable results. In these analyses, also the electrode sizes (radii, area) are determined.

Reliability of the diffusion coefficients can be increased by using data from such different diffusion conditions and, additionally, those from the conceptually totally independent PGSE NMR technique which does not rely on the measurement of Faradaic currents at all. Thus, it does not require knowledge about the details of the electrode reaction. Among other situations, correct diffusion coefficients are important for kinetic interpretations of cyclic voltammograms, which depend on the ratio $k_s/\sqrt{D}$, with k_s being the heterogeneous electron transfer rate constant. Determination of k_s thus critically depends on correctness of D.

Acknowledgments The authors thank Jürgen Heinze, Universität Freiburg, and Gunther Wittstock, Universität Oldenburg, for discussions. We are indebted to Jörg Henig and David Degler, Universität Tübingen, for preliminary experiments. Adrian Ruff thanks the Universität Tübingen for an LGFG fellowship.

References

1. Speiser B (2003) Linear sweep and cyclic voltammetry. In: Bard AJ, Stratmann M, Unwin P (eds) Encyclopedia of electrochemistry, vol. 3. Instrumentation and electroanalytical chemistry. Wiley-VCH, Weinheim, pp 81–104
2. Speiser B (2004) Methods to investigate mechanisms of electroorganic reactions. In: Bard AJ, Stratmann M, Schäfer H (eds) Encyclopedia of electrochemistry, vol 8, Organic electrochemistry. Wiley-VCH, Weinheim, pp 1–23
3. Heinze J (1991) Angew Chem 103:175–177, Angew Chem Int Ed Engl 30:170–171
4. Heinze J (1993) Angew Chem 105:1327–1349, Angew Chem Int Ed Engl 32:1268–1288
5. Nicholson RS, Shain I (1964) Anal Chem 36:706–723
6. Kakihana M, Ikeuchi H, Satô GP, Tokuda K (1980) J Electroanal Chem 108:381–383
7. Kakihana M, Ikeuchi H, Satô GP, Tokuda K (1981) J Electroanal Chem 117:201–211
8. Winlove CP, Parker KH, Oxenham RKC (1984) J Electroanal Chem 170:293–304
9. Baranski AS, Fawcett WR, Gilbert CM (1985) Anal Chem 57:166–170
10. Lawson DR, Whiteley LD, Martin CR, Szentirmay MN, Song JI (1988) J Electrochem Soc 135:2247–2253
11. Whiteley LD, Martin CR (1989) J Phys Chem 93:4650–4658
12. Amatore C, Azzabi M, Calas P, Jutand A, Lefrou C, Rollin Y (1990) J Electroanal Chem 288:45–63
13. Baur JE, Wightman RM (1991) J Electroanal Chem 305:73–81
14. Denuault G, Mirkin MV, Bard AJ (1991) J Electroanal Chem 308:27–38
15. Kulesza PJ, Faulkner LR (1993) J Am Chem Soc 115:11878–11884
16. Jung Y, Kwak J (1994) Bull Korean Chem Soc 15:209–213
17. Collinson MM, Zambrano PJ, Wang H, Taussig JS (1999) Langmuir 15:662–668

18. Evans RG, Klymenko OV, Saddoughi SA, Hardacre C, Compton RG (2004) J Phys Chem B 108:7878–7886
19. Lewera A, Miecznikowski K, Chojak M, Makowski O, Golimowski J, Kulesza PJ (2004) Anal Chem 76:2694–2699
20. Han LM, Suo QL, Luo MH, Zhu N, Ma YQ (2008) Inorg Chem Commun 11:873–875
21. Chanfreau S, Cognet P, Camy S, Condoret J-S (2007) J Electroanal Chem 604:33–40
22. Guo Y, Kanakubo M, Kodama D, Nanjo H (2010) J Electroanal Chem 639:109–115
23. Menshykau D, O'Mahony AM, Cortina-Puig M, del Campo FJ, Muñoz FX, Compton RG (2010) J Electroanal Chem 647:20–28
24. Shoup D, Szabo A (1982) J Electroanal Chem 140:237–245
25. Gritzner G, Kůta J (1984) Pure Appl Chem 56:461–466
26. Sun H, Chen W, Kaifer AE (2006) Organometallics 25:1828–1830
27. Dümmling S, Eichhorn E, Schneider S, Speiser B, Würde M (1996) Curr Sep 15:53–56
28. Metrohm, Herisau/CH: Electrode tips for rotating disk electrode (RDE), technical document no. 8.109.8002ML
29. Gollas B, Krauß B, Speiser B, Stahl H (1994) Curr Sep 13:42–44
30. Kuwana T, Bublitz DE, Hoh G (1960) J Am Chem Soc 82:5811–5817
31. Amatore C, Savéant JM (1978) J Electroanal Chem 86:227–232
32. Amatore C, Savéant JM (1979) J Electroanal Chem 102:21–40
33. Zara AJ, Machado SS, Bulhões LOS, Benedetti AV, Rabockai T (1987) J Electroanal Chem 221:165–174
34. Cassoux P, Dartiguepeyron R, Fabre P-L, de Montauzon D (1985) Electrochim Acta 30:1485–1490
35. Scholl H, Sochaj K (1989) Electrochim Acta 34:915–928
36. Clark ME, Ingram JL, Blakely EE, Bowyer WJ (1995) J Electroanal Chem 385:157–162
37. Jacob SR, Hong Q, Coles BA, Compton RG (1999) J Phys Chem B 103:2963–2969
38. Stejskal EO, Tanner JE (1965) J Chem Phys 42:288–292
39. Cohen Y, Avram L, Frish L (2005) Angew Chem 117:524–560, Angew Chem Int Ed 44:520–554
40. Bao D, Millare B, Xia W, Steyer BG, Gerasimenko AA, Ferreira A, Contreras A, Vullev VI (2009) J Phys Chem A 113:1259–1267
41. Einstein A (1906) Ann Phys 19:289–306
42. Valencia DP, González FJ (2011) Electrochem Commun 13:129–132
43. Tsierkezos NG (2007) J Solution Chem 36:289–302
44. Bulhões LOS, Chum HL, Soria D, Rabockai T (1978) In: Neves EA, Rabockai T (eds) Proc 1st Simp Bras Eletroquim Eletroanal, pp 78–84
45. Feng G, Xiong Y, Wang H, Yang Y (2008) Electrochim Acta 53:8253–8257
46. Reiter J, Vondrák J, Mička Z (2005) Electrochim Acta 50:4469–4476
47. Benedetti AV, Zara AJ, Spinola Machado S, Bulhões LOS (1982) In: Proc 3rd An Simp Bras Eletroquim Eletroanal, pp. 385–390
48. Scholl H, Sochaj K (1990) Electrochim Acta 35:93–94
49. Tsierkezos NG, Ritter U (2010) J Appl Electrochem 40:409–417
50. Leventis N, Chen M, Gao X, Canalas M, Zhang P (1998) J Phys Chem B 102:3512–3522
51. Diaz AF, Baier M, Wallraff GM, Miller RD, Nelson J, Pietro W (1991) J Electrochem Soc 138:742–747
52. Neghmouche NS, Khelef A, Lanez T (2010) Res J Pharm Biol Chem Sci 1:76–82
53. Nafady A, McAdam CJ, Bond AM, Moratti SC, Simpson J (2009) J Solid State Electrochem 13:1511–1519
54. Cooper JB, Bond AM (1991) J Electroanal Chem 315:143–160
55. Salmon A (2001) Synthese und Elektrochemie funktioneller Ferrocenyl- und Multiferrocenyl-Verbindungen. Ph.D. thesis, Univ. Bielefeld, Germany. URL http://bieson.ub.uni-bielefeld.de/volltexte/2003/347/pdf/0015.pdf
56. Lide DR (ed) (1995) Handbook of Organic Solvents. CRC, Boca Raton